Pergamon

PII S1359-6454(96)00158-9

Acta mater. Vol. 45, No. 1, pp. 331–341, 1997

Published by Elsevier Science Ltd

1359-6454/97 $17.00 + 0.00

NOTABLE HYDRIDING PROPERTIES OF A NANOSTRUCTURED COMPOSITE MATERIAL OF THE Mg_2Ni-H SYSTEM SYNTHESIZED BY REACTIVE MECHANICAL GRINDING

S. ORIMO, H. FUJII† and K. IKEDA

Faculty of Integrated Arts and Sciences, Hiroshima University, Higashi-Hiroshima 739, Japan

(Received 15 February 1996; accepted 3 March 1996)

Abstract—The intermetallic compound Mg_2Ni was mechanically ground under a hydrogen atmosphere to synthesize a nanostructured composite material that is composed of nanocrystalline intra-grain and disordered inter-grain regions. Both the thermal and magnetic analyses confirmed that a volume fraction of the latter region increases twenty times as much as that in the initial compound, nearly 30%, by grinding for only 60 min. As a result of this structural modification, notable hydriding properties emerged; the dissolved hydrogen content reaches up to 1.6 wt% ($Mg_2NiH_{1.8}$) without changing the crystal structure (Mg_2Ni type) of the nanocrystalline intragrain region, and the cooperative dehydriding reaction between both the regions occurs even at 413 K. The hydriding properties are most likely reversible in the temperature ranges below 473 K, above which the disordered inter-grain region transforms into a crystalline phase. *Copyright © 1996 Acta Metallurgica Inc.*

1. INTRODUCTION

Nanocrystalline materials [1] have drawn much scientific and technological interest in recent years [2, 3]. Since a large number of atoms locate at interfaces of nanometre-scale crystallites, the nanocrystalline materials show some unusual physical properties such as depression of the melting temperatures, formation of metastable phases and rapid diffusion of elemental substitutions, and so on [2, 3].

Hydriding properties of these nanocrystalline materials are also different from those of the conventional crystalline or amorphous ones on both the thermodynamic and kinetic aspects, as reported by Mütschele and Kirchheim [4]. One of the hydriding properties is an increase of hydrogen solubility as reported on gas-condensed nanocrystalline Pd [5, 6]. The origin of this phenomenon has been in controversy, but it seems to be due to an enhanced hydriding ability in the near-surface region of each crystallite of Pd [7–9]. Another is that hydrogen diffusivity in the nanocrystalline Pd or transition-metal alloys depends on the hydrogen content in grain boundaries [4, 6, 10–12]. A model in which hydrogen diffuses in a heterogeneous region composed of crystalline and amorphous structures was presented to give an explanation of the experimental results [13]. Moreover, improved kinetics in the hydriding process have been reported on nanocrystalline compounds such as Mg_2Ni, $LaNi_5$ and TiFe formed by the mechanical processing [14–17].

The above results suggest that the hydriding properties of nanocrystalline materials are dominantly affected by disordered regions at interfaces of nanometre-scale crystallites, which are a large volume fraction in nanocrystalline materials [18, 19]. In this sense, a nanocrystalline material can be regarded as a nanostructured composite material composed of the nanocrystalline intra-grain and disordered inter-grain regions. We believe that investigations for improving the hydriding properties of a nanocrystalline material should be closely linked with the volume fraction and its structural properties of the latter region.

Recently we have reported [20] the hydriding properties of the nanostructured composite material of the Mg_2Ni system at low temperatures; its hydrogen content reaches up to 1.6 wt% ($Mg_2NiH_{1.8}$) without changing the crystal structure of the intra-grain Mg_2Ni phase, and the dehydriding reaction occurs even at 440 K. On synthesizing this nanostructured composite material, the reactive mechanical grinding under a hydrogen atmosphere has been applied. This processing has already been applied to ZrNi-H [21, 22] and TiNi-H systems [23]. The first of the advantages is that many kinds of composite particles, composed of the crystalline and amorphous structures, could be formed by controlling hydrogen pressure [22]. The second is the appearance of an *in situ* activation effect for the

†To whom all correspondence should be addressed.

hydriding reaction by a continuous creation of active surfaces.

The aim in this paper is to clarify a close relation between the hydriding properties and the nanometre-scale structural properties on the Mg_2Ni-H system mechanically ground under a hydrogen atmosphere. In particular, we focus our attention on the disordered inter-grain region, which could improve the hydriding properties of the nanostructured composite material of the Mg_2Ni-H system.

2. EXPERIMENTAL PROCEDURES

2.1. Sample preparation

The initial compound Mg_2Ni was supplied from the Mazda Motor Corporation, and it contains small amounts of pure Mg and $MgNi_2$. Both the initial compound of 1 g of around 300 μm in size, and 20 steel balls of 7 mm in diameter (weight ratio 1:30) were placed in a steel vial of 30 cc volume. The vial, which was equipped with a connection valve for evacuation or introduction of hydrogen, was directly degassed for 720 min (12 h) below 0.01 Pa. Then, high-purity hydrogen (7 N) of 1.0 MPa (total amount of nearly 260 cc) was introduced into it. The initial compound was mechanically ground using a planetary ball mill apparatus (Fritsch P7) with 400 rpm for periods from 5 to 4800 min (80 h) at ambient temperature.

In this work, we pay attention to avoiding impurity effects on the hydriding and structural properties of the samples as far as possible. Therefore, the material and shape for the vial were carefully selected, so as to lower the amount of elemental Fe contaminated during the grinding process (negligibly small, as shown in Fig. 1). In addition, the vial with the sample was directly degassed prior to the grinding under a high-purity hydrogen atmosphere and was always handled in an argon grove-box before and after grinding, so as to minimize the oxidation effect on the sample.

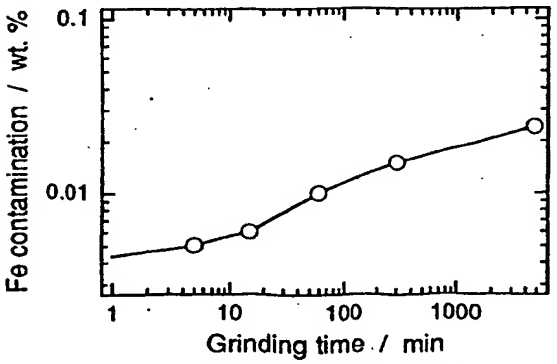

Fig. 1. Amount of the elemental Fe contaminated into the Mg_2Ni-H system ground under a hydrogen atmosphere, the value of which was examined by the induction coupled plasma (ICP) spectrometry.

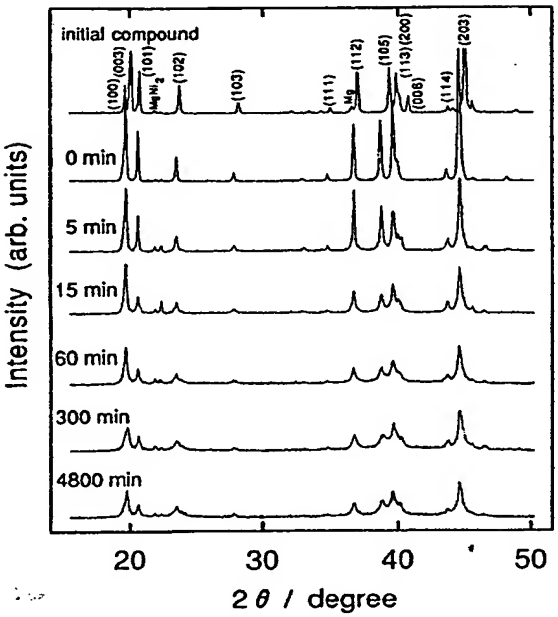

Fig. 2. X-ray diffraction profiles (Cu-Kα) of the Mg_2Ni-H system ground under a hydrogen atmosphere. The sample shown as "0 min" is the standard hydrogen dissolved $Mg_2NiH_{0.3}$ formed by a conventional hydrogenation for 720 min under a hydrogen pressure of 1.0 MPa.

2.2. Sample characterization

The hydriding and structural properties of the samples thus prepared were characterized by X-ray diffraction (Mac Science MXP3 and Rigaku 2500HF, Cu-Kα), thermal analyses (Seiko TG/DTA300), SEM (Hitachi S4100) and TEM (Hitachi H9000NAR) observation, BET (Brunauer-Emmett-Teller) adsorption examination (Shimazu GEMINI2360), and an examination of magnetic property (Toei-Kogyo VSM3-15).

The thermal analyses (thermogravimetry (TG) and differential thermal analysis (DTA)) were carried out under a purified argon atmosphere either in a heating condition at 5 K min^{-1} to 733 K or in an isothermal condition from 413 K to 453 K. Weights of the samples for the thermal analyses are 0.023–0.033 g. To prepare the TEM specimen, a thinning technique by a focused ion beam (FIB) was successfully employed (using Hitachi FB2000). The magnetic properties were examined by a vibrating sample magnetometer (VSM) under a magnetic field up to 16 kOe. Weights of the samples for the magnetic examination are 0.021–0.022 g.

3. RESULTS

3.1. Hydriding properties

X-ray diffraction profiles of the Mg_2Ni-H system are shown in Fig. 2. The standard hydrogen dissolved $Mg_2NiH_{0.3}$ [24–26] with hydrogen content of 0.3 wt% is formed by a conventional hydrogenation for

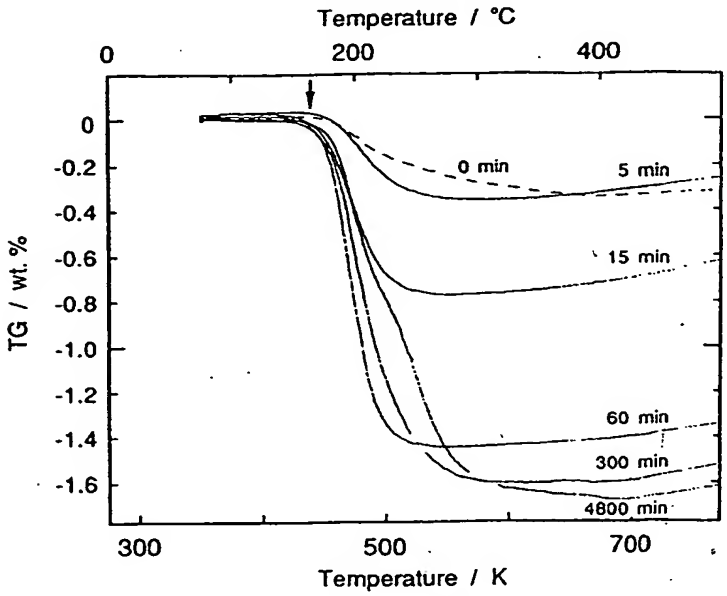

Fig. 3. Thermogravimetry (TG) profiles of the Mg_2Ni-H system ground under a hydrogen atmosphere.

720 min (12 h) under a hydrogen pressure of 1 MPa at room temperature. The diffraction peaks of $Mg_2NiH_{0.3}$ shift to a lower angle compared with those of the Mg_2Ni, especially the (00*l*) peaks. The profile corresponding to $Mg_2NiH_{0.3}$ becomes visible for the compound ground for only 5 min under a hydrogen atmosphere. Peak intensities are weakened by further grinding, but the peak positions remain unchanged. This indicates that the hydrogen dissolved $Mg_2NiH_{0.3}$ always exists in the intra-grain region of the compound, and that the volume fraction gradually reduces upon the grinding. No trace for hydride phases (Mg_2NiH_4), including both low and high temperature ones [24, 27–29], are found even after grinding for 4800 min (80 h).

The results of thermogravimetry (TG) shown in Fig. 3, however, indicate that the hydrogen content drastically increases by grinding up to 60 min. The hydrogen content almost saturates with grinding times longer than 60 min as shown in Fig. 4, and it finally reaches up to 1.6 wt% ($Mg_2NiH_{1.8}$). This hydrogen content exceeds 50% of the maximum values in chemically modified Mg_2Ni-H systems at ambient temperature—nearly 1.1 wt% [30, 31].

In spite of their different hydrogen contents, depending on the grinding time, the dehydriding reaction for all the samples starts to occur around 440 K (shown by an arrow in Fig. 3). A time-derivative of the dehydriding reaction, the so-called derivative themogravimetry (DTG), is shown in Fig. 5. This figure indicates that all the hydrogen in the compound ground for shorter than 60 min are dehydrogenated in the same temperature range as that for the hydrogen dissolved $Mg_2NiH_{0.3}$. This dehydriding temperature is much lower than that of low temperature (LT) phase of Mg_2NiH_4 which was confirmed to be 520–570 K in our experiments. Since no trace of the hydride phase is obtained in the X-ray diffraction profiles shown in Fig. 2, a dehydriding component around 520 K in the compound ground for 300 and 4800 min is due to the LT-Mg_2NiH_4 phase formed in the heating process in an argon atmosphere.

Judging from Figs 3 and 5, hydrogen in all the samples has a similar thermodynamic stability to that of hydrogen in the hydrogen dissolved $Mg_2NiH_{0.3}$. Thus, the increase of hydrogen content by grinding is regarded as an intensive increase of dissolved hydrogen into the Mg_2Ni system.

Dehydriding kinetics of the compound ground for 60 min were examined by isothermal thermogravimetry and are shown in Fig. 6. In this isothermal

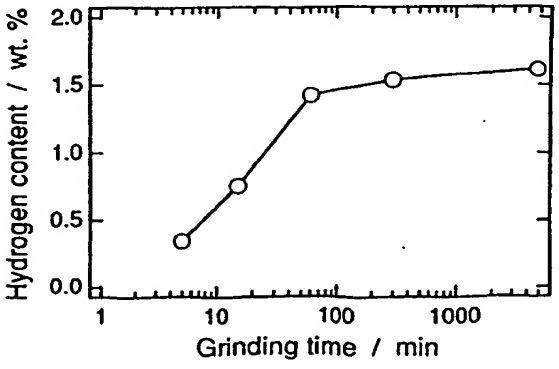

Fig. 4. Hydrogen content as a function of a grinding time in the Mg_2Ni-H system ground under a hydrogen atmosphere.

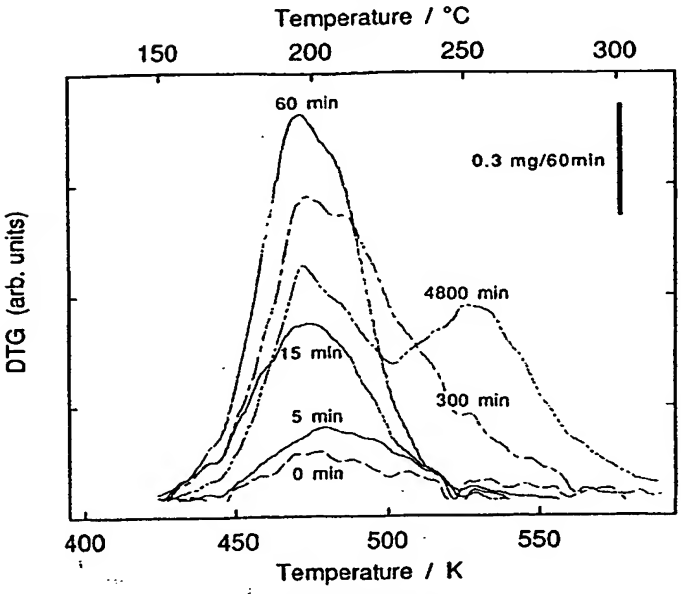

Fig. 5. Derivative themogravimetry (DTG) profiles of the Mg_2Ni-H system ground under a hydrogen atmosphere.

condition, the dehydriding reaction proceeds even at 413 K. At 453 K, 90% of dissolved hydrogen (1.3 wt%) in the sample is dehydrogenated within 30 min. An activation energy for the dehydriding reaction, which is calculated by the Arrhenius plot of reaction-rate constants (shown in Fig. 7), is nearly 130 kJ mol^{-1}. This value is comparable with that for Mg_2NiH_4 at higher temperature ranges around 500 K [32].

3.2. *Structural properties*

Various kinds of structural analyses were carried out to explain the notable hydriding properties as described in Section 3.1.

First we tried the BET adsorption examination and the SEM observation. Figure 8 shows the relation between the specific surface area and the hydrogen content of the samples. In a grinding process shorter than 15 min, the hydrogen content increases linearly with increasing specific surface area. This probably corresponds to the milling effect reported by Aoki *et al.* [33]. In a grinding process from 15 to 60 min, however, the hydrogen content increases more rapidly than expected from the increase of the specific surface area. Any morphological change is not recognized in this grinding process, as is evident from the SEM observation in Fig. 9, in which both the samples are composed of particles of size of less than several micrometres. In this way, the differences of hydrogen content shown in Fig. 3 cannot be understood from either the surfacial or the morphological features of the samples.

We therefore claim that the rapid increase of the hydrogen content is caused by a high density

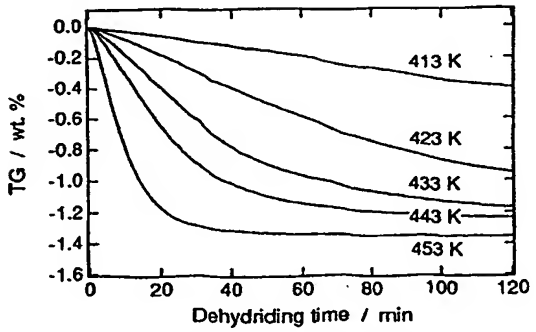

Fig. 6. Dehydriding kinetics of the Mg_2Ni-H system ground for 60 min under a hydrogen atmosphere.

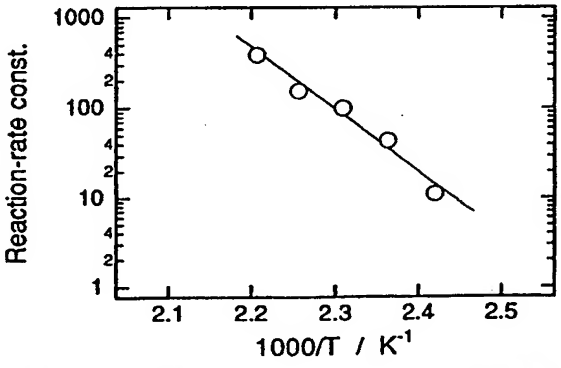

Fig. 7. Arrhenius plot of the reaction-rate constants in dehydriding reaction of the Mg_2Ni-H system ground for 60 min under a hydrogen atmosphere. The reaction-rate constants are determined using Fig. 6.

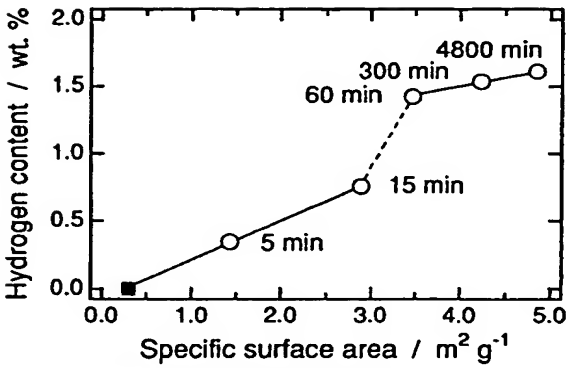

Fig. 8. Hydrogen content as a function of a specific surface area of the Mg_2Ni-H system ground under a hydrogen atmosphere. A closed square represents the value for the initial compound.

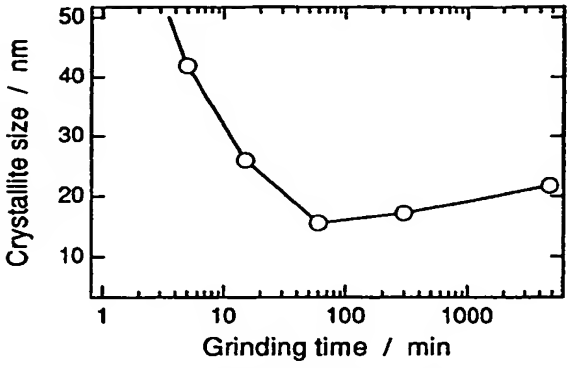

Fig. 10. Size transformation of the crystallites of the Mg_2Ni-H system ground under a hydrogen atmosphere.

hydrogen occupation in the disordered inter-grain region around nanometre-scale crystallites of the hydrogen dissolved $Mg_2NiH_{0.3}$, mainly formed during the grinding from 15 to 60 min.

Next the examinations concerning the nanometre-scale crystallites were carried out. Figure 10 shows the size transformation of the crystallites by grinding. The sizes of crystallites were analysed from the peak broadening of X-ray diffraction shown in Fig. 2,

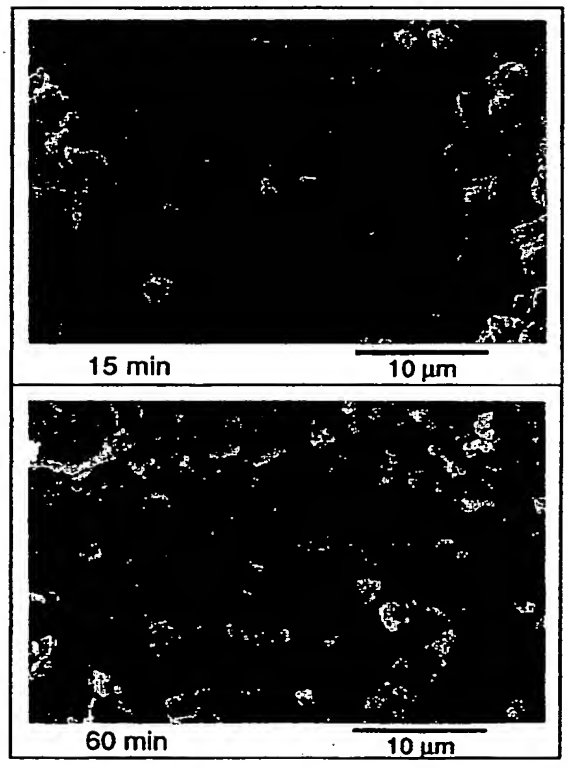

Fig. 9. SEM images of the Mg_2Ni-H system ground for 15 min and 60 min under a hydrogen atmosphere.

using the Wilson method [34] (using the application software of the X-ray diffraction apparatus, Rigaku 2500HF). In this method, the size and lattice strain effects of the crystallites on the broadening of the X-ray diffraction peak are individually estimated by using an approximation of both the Cauchy and Gaussian functions, respectively. As a result of the analyses, the average crystallite sizes are found to reduce down to 16 nm by grinding for 60 min. A slight increase of the sizes by over grinding may relate to a coagulation of the particles. We could find almost no lattice strain in the crystallites of all the samples ground under a hydrogen atmosphere.

One of the high resolution TEM (HRTEM) images of the compound ground for 60 min is shown in Fig. 11 [35]. This lattice image indicates that the sample is composed of the equiaxed Mg_2NiH_x ($x < 0.3$) without sharp boundaries. The average crystallite size is estimated to be 15 nm or less. This value well agrees with the estimation from the peak broadening in X-ray diffraction shown in Fig. 10. Here, we would like to emphasize that all our images were obtained from the inner areas of each particle thinned by the focused ion beam (FIB) cutting technique [35–37]. Conventionally for the TEM observation of the nanometre-scale structure of particles, only edge areas of particles have been examined so far.

Finally, the magnetization curves of the samples were measured to estimate the volume fraction of the disordered inter-grain region from the precipitation amount of elemental Ni. The results obtained are shown in Fig. 12. The hydrogen dissolved $Mg_2NiH_{0.3}$ exhibit a weak diamagnetic behaviour [38]. Through grinding, however, a super-paramagnetic component [39, 40] gradually appears, which is attributed to the formation of micro-clustered elemental Ni, probably in the precipitation range of less than several nanometres. This directly supports the increment of the disordered inter-grain region, at which the initial Mg_2Ni type atomistic structure is deformed by an accumulation of the external energy of the grinding. The magnetic moments at the magnetic field of

16 kOe are summarized in Table 1. On the basis of the change of magnetic moment from 0 to 5 min, it is deduced that the volume fraction of the disordered inter-grain region of the compound ground for 15 or 60 min increases nearly 7 or 18 times as much as that for 5 min, respectively. The magnetic moment of the compounds ground for longer than 60 min were almost constant.

4. DISCUSSION

Experimentally it was revealed that the formation of the disordered inter-grain region causes an intensive increase of the dissolved hydrogen into Mg_2Ni. Here, we estimate an absolute volume fraction of the disordered inter-grain region (V_f) and its dissolved hydrogen content (H_c wt%). In the

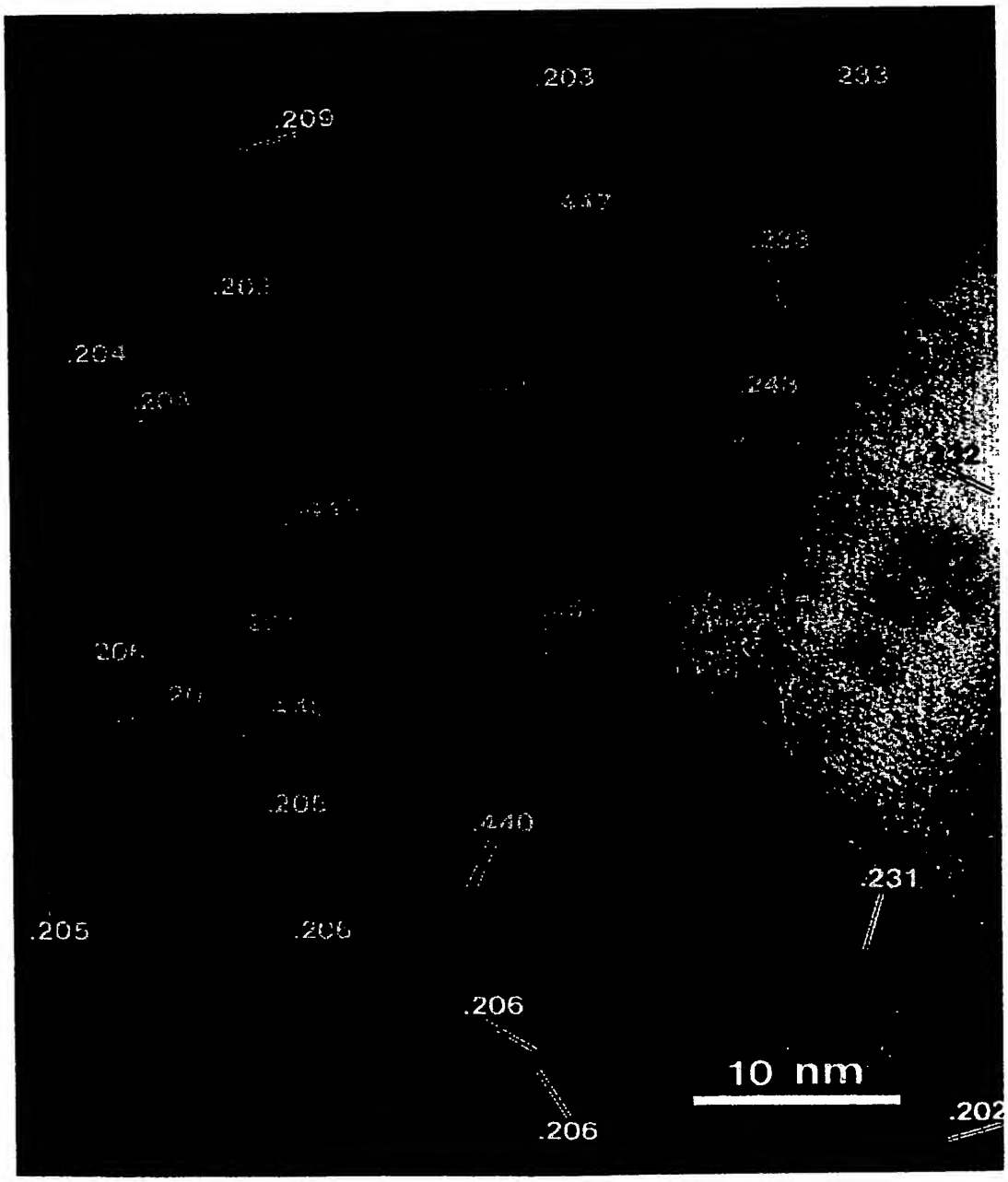

Fig. 11. High resolution TEM (HRTEM) images of the Mg_2Ni-H system ground for 60 min under a hydrogen atmosphere [35].

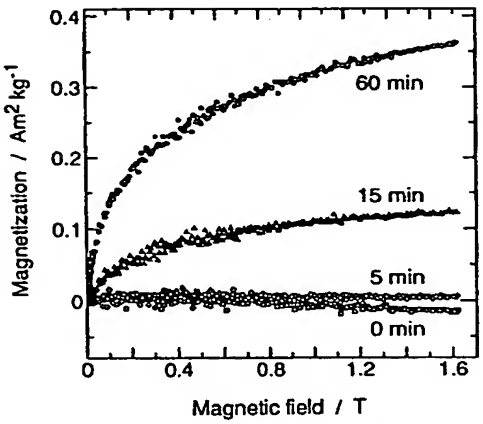

Fig. 12. Magnetization curve of the Mg_2Ni-H system ground under a hydrogen atmosphere.

compound ground for 60 min, the dissolved hydrogen content (1.4 wt% from Fig. 2) is expressed as follows;

$$1.4\ \text{wt\%} = (1 - V_f(60\ \text{min})) \times 0.3\ \text{wt\%} + V_f(60\ \text{min}) \times H_c\ \text{wt\%}. \quad (1)$$

The first term on the right hand side expresses the dissolved hydrogen in the intra-grain region (always 0.3 wt% due to the presence of the $Mg_2NiH_{0.3}$ phase), and the second one expresses that in the inter-grain region. Setting the volume fraction of the disordered inter-grain region (V_f(60 min)) to 0.1, 0.3 and 0.5, the dissolved hydrogen content in the disordered inter-grain region (H_c) becomes 11.5, 4.0 and 2.5, respectively. Using the following equation [4],

$$V_f = 3 \times I_t/C_s \quad (2)$$

where I_t and C_s represent the thickness of the inter-grain region and the average crystallite size shown in Fig. 10, respectively: the value of V_f(60 min) is obtained to be around 0.3 for $I_t = 1.5$ nm. In this case the dissolved hydrogen content in the disordered inter-grain region (H_c) reaches 4.0 wt%. This value is almost the same as that in the Mg_2NiH_4 phase, and is most probable. We could find from this estimation that around 85% of hydrogen in the compound ground for 60 min, was in the disordered inter-grain region.

Table 1. Magnetic moment at 16 kOe of the Mg_2Ni-H system ground under a hydrogen atmosphere

Grinding time (min)	Magnetic moment (10^{-3} emu g^{-1})
0†	−1.5‡
5	0.57
15	12
60	36

†The standard hydrogen dissolved $Mg_2NiH_{0.3}$ formed by a conventional hydrogenation for 720 min under a hydrogen pressure of 1 MPa.
‡Weak diamagnetic behaviour.

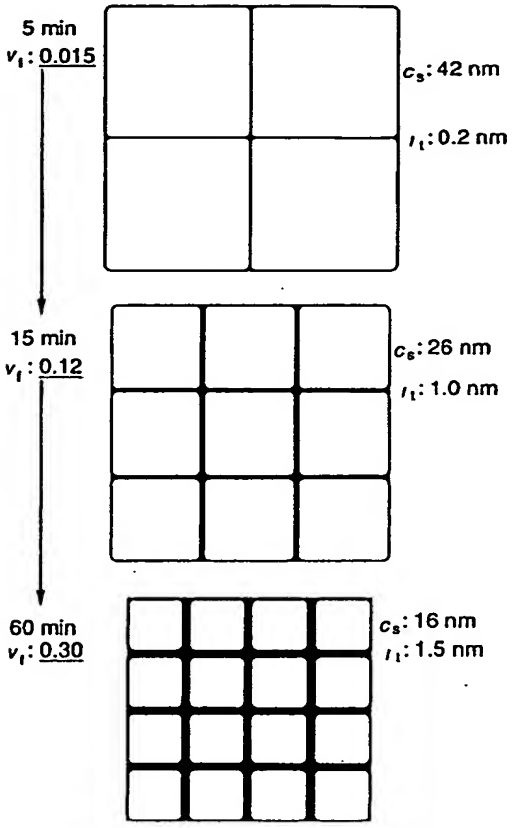

Fig. 13. Schematic figure for the nanostructured composite materials of the Mg_2Ni-H system ground under a hydrogen atmosphere. Here C_s, I_t and V_f represent average crystallite size, thickness of the inter-grain region and volume fraction of the disordered inter-grain region, respectively.

Grinding-time dependence of V_f is calculated in a similar way by fixing this value (4.0 wt%) of H_c. As a result, V_f of the compound ground for 5 and 15 min is deduced to be 0.015 and 0.12, respectively. These features are schematically shown in Fig. 13. It is noted that the grinding-time dependence of the volume fraction of the disordered inter-grain region agrees satisfactorily well with that independently estimated from the magnetic moment, as shown in Fig. 12. That is, V_f of the compound ground for 15 and 60 min increases by nearly 8 and 20 times as large as that for 5 min, respectively.

The formation of the disordered inter-grain region was not detected in the X-ray diffraction profiles (Fig. 2), because the interface thickness is less than a few nanometres. It may result in only an increase of diffuse background intensities [7, 41, 42].

To clarify the thermal stability of the disordered inter-grain region, we carried out the thermal analyses of the Mg_2Ni(-H) system ground for 4800 min (80 h) under an argon atmosphere. It was

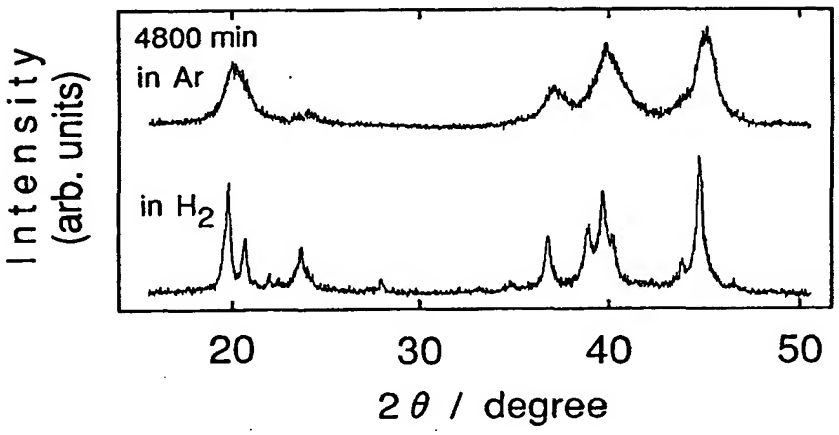

Fig. 14. X-ray diffraction profiles (Cu-Kα) of Mg_2Ni ground for 4800 min under an argon atmosphere. For a comparison, the profile of the Mg_2Ni-H system ground for 4800 min under a hydrogen atmosphere (the same sample as shown in Fig. 2) is also shown below.

confirmed from the peak broadening of X-ray diffraction (Fig. 14) that the average crystallite size of this sample is much less than 10 nm, and the volume fraction of the inter-grain region exceeds more than 50% of the total volume using equation (2). In addition, the residual lattice strain (local and non-uniform deviation of lattice constant) of more than 0.4% was also found to exist in the crystallites. Therefore we believe that the structural properties of this sample, as a whole, represent those for the disordered inter-grain region of the compound ground under a hydrogen atmosphere. Thermal analyses of an as-ground sample are shown in Fig. 15(a). Any thermogravimetrical and thermal reactions are not detected in the sample ground under an argon atmosphere. After the conventional hydrogenation for 60 min under a hydrogen pressure of 1 MPa, the similar thermal analyses were carried out and the results are shown in Fig. 15(b). In this figure, there are two weight losses in the TG profile

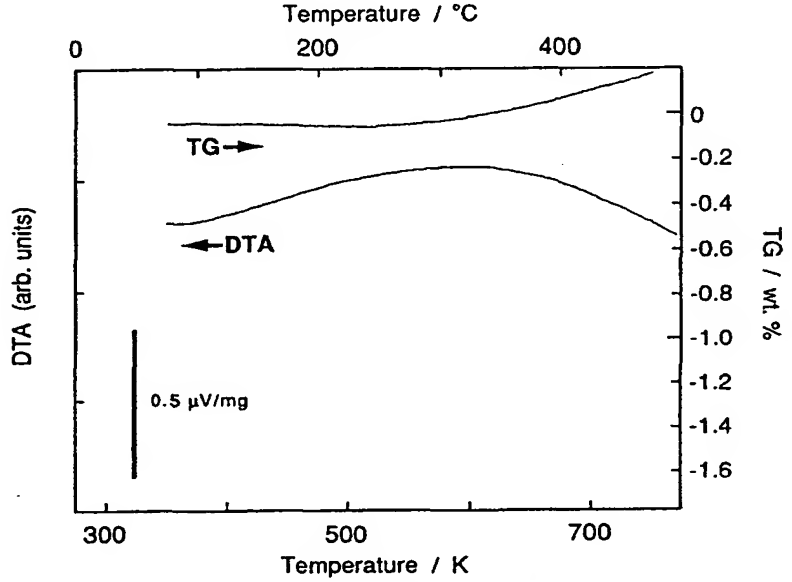

Figure 15(a) *caption opposite*

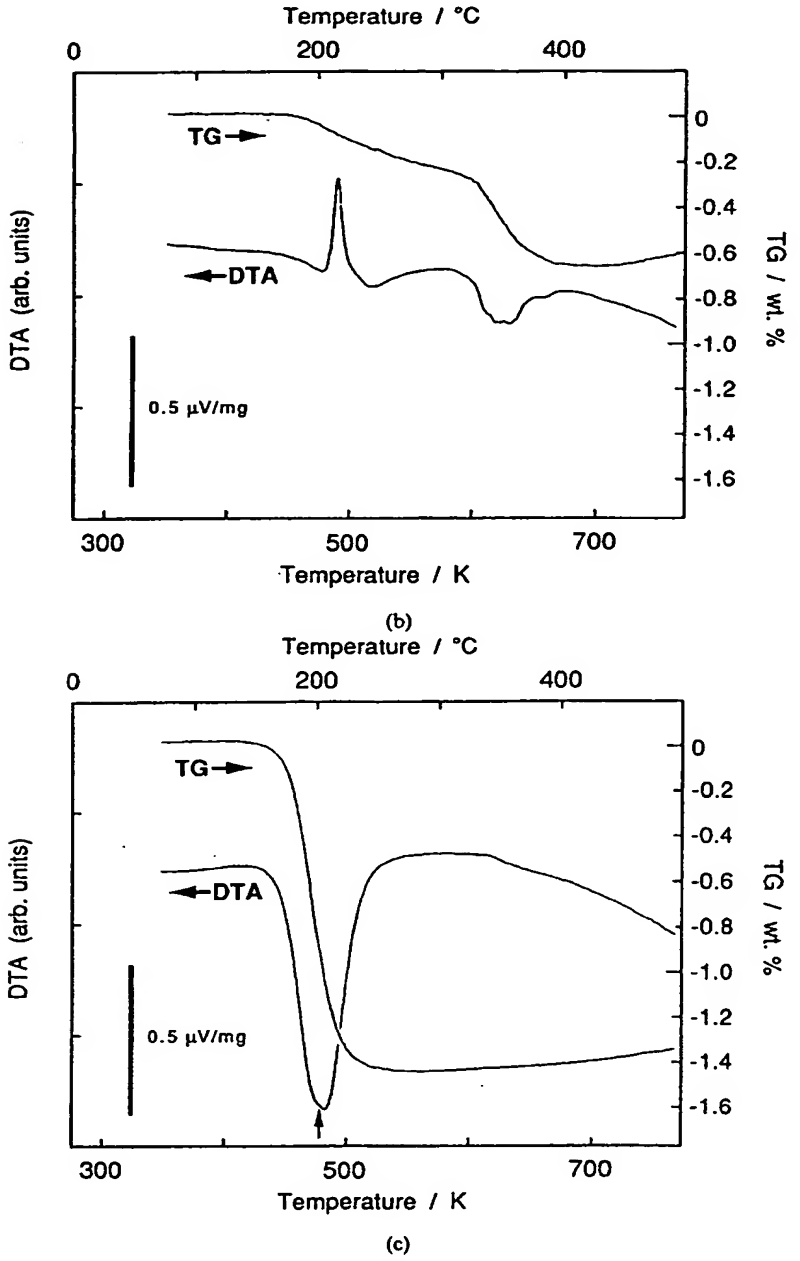

Fig. 15. Thermogravimetry and differential thermal analysis (TG/DTA) of (a) Mg_2Ni ground for 4800 min under an argon atmosphere, and (b) its hydrogenated sample for 60 min under a hydrogen pressure of 1 MPa. Figure 15(c) corresponds to a TG/DTA profile of the Mg_2Ni-H system ground for only 60 min under a hydrogen atmosphere (the same sample as shown in Fig. 2). The upper direction shows the exothermic reaction in each figure.

and a sharp exothermic as well as two broad endothermic reactions in the DTA profile. The endothermic reactions are attributed to the dehydriding reaction of the stable hydride phases such as LT- and HT-Mg_2NiH_4, in addition to that of $Mg_2NiH_{0.3}$.

Here, we will focus on the sharp exothermic reaction at 473 K in Fig. 15(b). Quite a tiny trace of the same reaction was found in the compound ground for 60 min under a hydrogen atmosphere (shown by an arrow in Fig. 15(c)). This exothermic reaction indicates that the disordered inter-grain region crystallizes into the hydride phase (LT-Mg_2NiH_4) at this temperature range. By the formation of this hydride phase, the dehydriding reaction is transferred

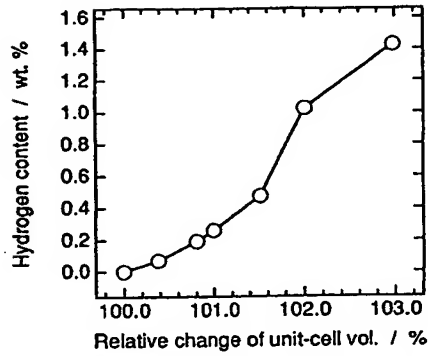

Fig. 16. Hydrogen content in the whole of the samples as a function of a relative change of the unit-cell volume of the intra-grain Mg_2Ni phase in the dehydriding process.

to higher temperatures around 520 K. In other words, this implies that the reversible hydriding and dehydriding reaction without changing the atomistic structure of the disordered inter-grain region is only realized below 473 K.

Indeed the reversibility was examined using the sample which is first ground for 60 min under a hydrogen atmosphere. After the dehydrogenation at 453 K (shown in Fig. 6), the sample was re-hydrogenated at 333 K. Then, the hydrogen content reaches up to 1.4 wt% which is almost the same as that for the first run. We can therefore confirm that the nanostructured composite material essentially possesses the reversibility to react with hydrogen.

We finally discuss the cooperative dehydriding reaction of the Mg_2Ni-H system ground for 60 min under a hydrogen atmosphere. Figure 16 shows the whole hydrogen content as a function of relative change of the unit-cell volume of the intra-grain Mg_2Ni phase in the samples dehydrogenated for 120 min at each temperature shown in Fig. 6. The unit-cell volume of each sample was calculated from the lattice constant shown in Table 2. The full expansion of unit-cell volume, nearly 3%, corresponds to the formation of $Mg_2NiH_{0.3}$. The relative lattice shrinkage directly shows the dehydriding reaction from the intra-grain region. As is evident from Fig. 16, the dehydrogenated amount from the compound, where around 85% of hydrogen was initially in the disordered inter-grain region as mentioned above, is almost proportional to that from the intra-grain Mg_2Ni phase. This implies an appearance of the cooperative dehydriding process between the intra- and inter-grain regions. That is, the lattice shrinkage upon the dehydriding of the intra-grain region most likely leads to the thermal instabilities of hydrogen in the disordered inter-grain region, and promotes the dehydriding reaction of the compound. This phenomenon should be examined in more details both from the scientific and technological aspects.

In addition to the various examinations described in this paper, the small angle neutron scattering (SANS) measurements have clarified a spatial inhomogeneity of hydrogen (deuterium) concentration between the intra- and inter-grain regions [43]. Nuclear magnetic resonance (proton NMR) [44–46] is also in progress to obtain information on complex-structures of Mg-Ni-H and hydrogen diffusivities mainly in the disordered inter-grain region.

5. CONCLUSIONS

The dissolved hydrogen content in Mg_2Ni synthesized by reactive mechanical grinding under a hydrogen atmosphere reaches up to 1.6 wt% ($Mg_2NiH_{1.8}$), without changing the crystal structure of the intra-grain Mg_2Ni phase. Moreover, the cooperative dehydriding reaction between the intra- and inter-grain regions occurs even at 413 K. These phenomena originate from the formation of a nanostructured composite material which is composed of the nanocrystalline intra-grain and disordered inter-grain regions. The volume fraction and its hydrogen content of the latter region in the compound ground for 60 min are estimated to be 30% and 4.0 wt%, respectively. Since the disordered inter-grain region transforms into the crystalline phase at 473 K, the reversibility to react with hydrogen is most likely realized below this temperature.

Acknowledgements—This work was supported by a fund for Fundamental Technology from the Hiroshima Prefecture and by a Grant-in-Aid for Scientific Research from the Ministry of Education, Science and Culture of Japan. The authors acknowledge Dr H. Watanabe and Mr Y. Yamagata of the Western Hiroshima Prefecture Industrial Research Institute and Mr K. Higuchi of the Hiroshima Prefectural Joint Research Center for Advanced

Table 2. Lattice constants and unit-cell volumes of the intra-grain Mg_2Ni region in the samples dehydrogenated for 120 min at each temperature

Sample	Lattice constant (nm)		Unit-cell volume (nm^3)
Initial compound	a = 0.521 (0)	c = 1.32 (3)	0.311 (0)
as ground for 60 min	0.524 (1)	1.34 (7)	0.320 (4)
dehydrogenated at			
413 K	0.523 (1)	1.34 (0)	0.317 (5)
423 K	0.522 (9)	1.33 (4)	0.315 (9)
433 K	0.522 (2)	1.33 (0)	0.314 (1)
443 K	0.522 (0)	1.32 (9)	0.313 (6)
453 K	0.521 (3)	1.32 (7)	0.312 (3)

Technology, for valuable ICP and BET adsorption examination. The authors also acknowledge Mr T. Morishita of the Mazda Motor Corporation, for kindly supplying the initial compound. One of the authors (SO) is grateful for a PD Fellowship from the Japan Society for the Promotion of Science.

REFERENCES

1. R. Birringer, H. Gleiter, H.-P. Klein and P. Marquardt, *Phys. Lett.* **102A**, 365 (1984).
2. R. W. Siegel, *Physics Today* **10**, 64 (1993).
3. H. Gleiter, *Z. Metallkd.* **86**, 78 (1995).
4. T. Mütschele and R. Kirchheim, *Scr. metall.* **21**, 135 (1987).
5. T. Mütschele and R. Kirchheim, *Scr. metall.* **21**, 1101 (1987).
6. R. Kirchheim, T. Mütschele, W. Kieninger, H. Gleiter, R. Birringer and T. D. Koblé, *Mat. Sci. Eng.* **99**, 457 (1988).
7. J. A. Eastman, L. J. Thompson and B. J. Kestel, *Phys. Rev. B* **48**, 84 (1993).
8. P. G. Sanders, J. R. Weertman, J. G. Barker and R. W. Siegel, *Scr. metall.* **29**, 91 (1993).
9. R. J. Wolf, M. W. Lee and J. R. Ray, *Phys. Rev. Lett.* **73**, 557 (1994).
10. C. U. Maier and H. Kronmüller, *J. Less-Common Met.* **172–174**, 671 (1991).
11. J. Mössinger and M. Hirscher, *Z. Phys. Chem.* **183**, 13 (1994).
12. M. Hirscher, S. Zimmer and H. Kronmüller, *Z. Phys. Chem.* **183**, 51 (1994).
13. M. Hirscher, J. Mössinger and H. Kronmüller, *J. Alloys and Comp.* **231**, 267 (1995).
14. L. Zaluski, P. Tessier, D. H. Ryan, C. B. Doner, A. Zaluska, J. O. Ström-Olsen, M. L. Trudeau and R. Schulz, *J. Mater. Res.* **8**, 3059 (1993).
15. L. Zaluski, A. Zaluska and J. O. Ström-Olsen, *J. Alloys and Comp.* **217**, 245 (1995).
16. L. Zaluski, A. Zaluska, P. Tessier, J. O. Ström-Olsen and R. Schulz, *J. Alloys and Comp.* **217**, 295 (1995).
17. A. K. Singh, A. K. Singh and O. N. Srivastava, *J. Alloys and Comp.* **227**, 63 (1995).
18. X. Zhu, R. Birringer, U. Herr and H. Gleiter, *Phys. Rev. B* **35**, 9085 (1987).
19. K. Lu, R. Lück and B. Predel, *Acta metall. mater.* **42**, 2303 (1994).
20. S. Orimo and H. Fujii, *J. Alloys and Comp.* **232**, L16 (1996).
21. K. Aoki, A. Memezawa and T. Masumoto, *J. Mater. Res.* **8**, 307 (1993).
22. S. Orimo, H. Fujii and T. Yoshino, *J. Alloys and Comp.* **217**, 287 (1995).
23. M. S. El-Eskandarany, H. A. Ahmed, K. Sumiyama and K. Suzuki, *J. Alloys and Comp.* **218**, 36 (1995).
24. J. Schefer, P. Fischer, W. Hälg, F. Stucki, L. Schlapbach, J. J. Didisheim, K. Yvon and A. F. Andresen, *J. Less-Common Met.* **74**, 65 (1980).
25. D. Noréus and P. Werner, *Acta Chem. Scand. A* **36**, 847 (1982).
26. J. L. Soubeyroux, D. Fruchart, A. Mikou, M. Pezat and B. Darriet, *Mat. Res. Bull.* **19**, 895 (1984).
27. S. Ono, H. Hayakawa, A. Suzuki, K. Nomura, N. Nishimiya and T. Tabata, *J. Less-Common Met.* **88**, 63 (1982).
28. H. Hayakawa, Y. Ishido, K. Nomura, H. Uruno and S. Ono, *J. Less-Common Met.* **103**, 277 (1984).
29. D. Noréus and L. Kihlborg, *J. Less-Common Met.* **123**, 233 (1986).
30. H. Imamura, T. Takahashi, R. Galleguillos and S. Tsuchiya, *J. Less-Common Met.* **89**, 251 (1983).
31. F.-J. Liu, G. Sandrock and S. Suda, *Z. Phys. Chem.* **183**, 163 (1994).
32. Y. Osumi, *Hydrogen Storage Alloy—Its Properties and Applications*, Agne Technical Center, Tokyo (1993) (in Japanese), p. 161.
33. K. Aoki, H. Aoyagi, A. Memezawa and T. Masumoto, *J. Alloys and Comp.* **203**, L7 (1994).
34. H. P. Klug and L. E. Alexander, *X-ray Diffraction Procedures for Polycrystalline and Amorphous Materials* (second edition), A Wiley-Interscience Publication, New York (1974) p. 618.
35. Y. Kitano, Y. Fujikawa, N. Shimizu, S. Orimo, H. Fujii, T. Kamino and T. Yaguchi, *Intermetallics*, in press.
36. Y. Kitano, Y. Fujikawa, H. Takeshita, T. Kamino, T. Yaguchi, H. Matsumoto and H. Koike, *J. Electron Microsc.* **44**, 376 (1995).
37. Y. Kitano, Y. Fujikawa, T. Kamino, T. Yaguchi and H. Saka, *J. Electron Microsc.* **44**, 410 (1995).
38. M. Gupta and L. Schlapbach, *Topics in Applied Physics* (Edited by L. Schlapbach), Vol. 63, 67 *Hydrogen in Intermetallic Compounds I, II*, Springer, Berlin/Heidelberg (1992) p. 200.
39. C. P. Bean and I. S. Jacobs, *J. Appl. Phys.* **27**, 1448 (1956).
40. I. Nagy, I. Bakonyi, A. Lovas, E. Tóth-Kádár, K. Tompa, M. Hossó, Á. Cziráki and B. Fogarassy, *J. Less-Common Met.* **167**, 283 (1991).
41. M. R. Fitzsimmons, J. A. Eastman, M. Müller-Stach and G. Wallner, *Phys. Rev. B* **44**, 2452 (1991).
42. J. A. Eastman, M. R. Fitzsimmons and L. J. Thompson, *Phil. Mag. B* **66**, 667 (1992).
43. S. Orimo, H. Seto, K. Ikeda, M. Nagao and H. Fujii, *Physica B*, in press.
44. S. Hayashi, K. Hayamizu and O. Yamamoto, *J. Chem. Phys.* **79**, 2308 (1983).
45. J. Senegas, M. Y. Song, M. Pezat and B. Darriet, *J. Less-Common Met.* **129**, 317 (1987).
46. S. Hayashi and K. Hayamizu, *J. Less-Common Met.* **155**, 31 (1989).